Langmuir Article

pubs.acs.org/Langmuir

Janus Microgels Produced from Functional Precursor Polymers

Sebastian Seiffert, Mark B. Romanowsky, and David A. Weitz*

School of Engineering and Applied Sciences and Department of Physics, Harvard University, 29 Oxford Street, Cambridge, Massachusetts 01238

Received May 10, 2010. Revised Manuscript Received August 4, 2010

Micrometer-sized Janus particles of many kinds can be formed using droplet microfluidics, but in existing methods, the microfluidic templating is strongly coupled to the material synthesis, since droplet solidification occurs through rapid polymerization right after droplet formation. This circumstance limits independent control of the material properties and the morphology of the resultant particles. In this paper, we demonstrate a microfluidic technique to produce functional Janus microgels from prefabricated, cross-linkable precursor polymers. This approach separates the polymer synthesis from the particle gelation, thus allowing the microfluidic droplet templating and the functionalization of the matrix polymer to be performed and controlled in two independent steps. We use microfluidic devices to emulsify semidilute solutions of cross-linkable, chemically modified or unmodified poly(*N*-isopropylacrylamide) precursors and solidify the drops via polymer-analogous gelation. The resultant microgel particles exhibit two distinguishable halves which contain most of the modified precursors, and the unmodified matrix polymer separates these materials. The spatial distribution of the modified precursors across the particles can be controlled by the flow rates during the microfluidic experiments. We also form hollow microcapsules with two different sides (Janus shells) using double emulsion droplets as templates, and we produce Janus microgels that are loaded with a ferromagnetic additive which allows remote actuation of the microgels.

Introduction

Janus particles are compartmentalized structures with two distinct sides of different chemistry, polarity, or surface modification;[1,2] they can be employed as powerful surfactants,[3,4] nano- or microsensors,[5−7] actuators in optical devices,[8] or as model systems to study self-assembly and dielectric phenomena.[9−11] An extraordinarily versatile and controllable method for the production of these useful materials is through the use of droplet microfluidics. The principle of this approach is to create a laminar coflowing stream of two curable liquids in a microchannel. Periodic break-up of this stream, induced by flow focusing with a third immiscible fluid (continuous phase), can produce monodisperse micrometer-sized Janus droplets at kilohertz rates. Subsequent curing or gelling of these droplets, typically achieved through rapid (photo)polymerization right after droplet formation, leads to Janus particles.

A striking advantage of the microfluidic approach is that particles are obtained with extremely low polydispersity and the size and shape of these particles can be controlled by the experimental parameters.[8] Hence, this technique has been used extensively to create Janus structures of various types and for multiple applications: Nisisako and colleagues fabricated charged, black-and-white-pigmented Janus particles and illustrated their actuation in electric fields.[8] They also demonstrated an approach for large-scale production of these particles. Yang and co-workers extended this work toward the formation of colored Janus particles, which can also be actuated in electric fields.[12] Kumacheva et al. produced bi- and triphasic particles from independent streams of different immiscible monomers.[13] Weitz and collaborators used microfluidic channels with spatially controlled wettability to obtain double emulsion droplets, serving as templates to fabricate bipolar microparticles[14] or microgels with an anisotropic, superparamagnetic functionalization.[15] Recently, Doyle and colleagues extended this work and presented an impressive way to fabricate anisotropic microparticles which have one of their sides loaded with superparamagnetic nanoparticles.[16] These authors also presented a thorough magnetic characterization of the resultant microparticles and demonstrated the ability to align these particles to one-dimensional superstructures by the application of external magnetic fields. However, all these previous approaches have one common, intrinsic limitation: since the microfluidic droplet templating and the subsequent polymerization are coupled within a single step, flexibility in independently controlling the material properties and the morphology of the resultant microparticles is limited. Therefore, many previous microfluidic approaches created Janus particles only with very coarse modifications of their two sides, either by nesting different

*seiffert@seas.harvard.edu; weitz@seas.harvard.edu.

(1) Perro, A.; Reculusa, S.; Ravaine, S.; Bourgeat-Lami, E.; Duguet, E. *J. Mater. Chem.* **2005**, *15*, 3745–3760.
(2) Walther, A.; Mueller, A. H. E. *Soft Matter* **2008**, *4*, 663–668.
(3) Glaser, N.; Adams, D. J.; Boeker, A.; Krausch, G. *Langmuir* **2006**, *22*, 5227–5229.
(4) Walther, A.; Hoffmann, M.; Mueller, A. H. E. *Angew. Chem., Int. Ed.* **2008**, *47*, 711–714.
(5) Takai, H.; Shimizu, N. *Langmuir* **1997**, *13*, 1865–1868.
(6) Behrend, C. J.; Anker, J. N.; Kopelman, R. *Appl. Phys. Lett.* **2004**, *84*, 154–156.
(7) Behrend, C. J.; Anker, J. N.; McNaughton, B. H.; Brasuel, M.; Philbert, M. A.; Kopelman, R. *J. Phys. Chem. B* **2004**, *108*, 10408–10414.
(8) Nisisako, T.; Torii, T.; Takahashi, T.; Takizawa, Y. *Adv. Mater.* **2006**, *18*, 1152–1156.
(9) Vanakaras, A. G. *Langmuir* **2006**, *22*, 88–93.
(10) Dendukuri, D.; Hatton, T. A.; Doyle, P. S. *Langmuir* **2007**, *23*, 4669–4674.
(11) Cayre, O.; Paunov, V. N.; Velev, O. D. *J. Mater. Chem.* **2003**, *13*, 2445–2450.
(12) Kim, S.-H.; Jeon, S.-J.; Jeong, W. C.; Park, H. S.; Yang, S.-M. *Adv. Mater.* **2008**, *20*, 4129–4134.
(13) Nie, Y.; Li, W.; Seo, M.; Xu, S.; Kumacheva, E. *J. Am. Chem. Soc.* **2006**, *128*, 9408–9412.
(14) Chen, C.-H.; Shah, R. K.; Abate, A. R.; Weitz, D. A. *Langmuir* **2009**, *25*, 4320–4323.
(15) Chen, C.-H.; Abate, A. R.; Lee, D.; Terentjev, E. M.; Weitz, D. A. *Adv. Mater.* **2009**, *21*, 3201–3204.
(16) Yuet, K. P.; Hwang, D. K.; Haghgooie, R.; Doyle, P. S. *Langmuir* **2010**, *26*, 4281–4287.

Scheme 1. UV-Induced Cross-Linking of Dimethylmaleimide (DMMI) Functionalized Polymers[a]

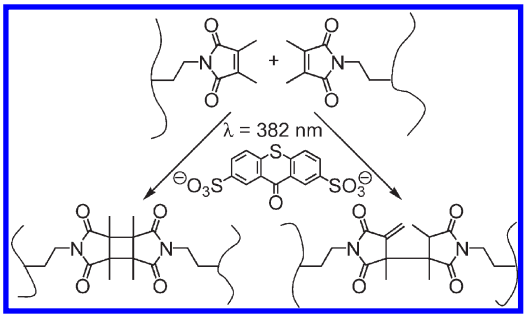

[a] Two isomeric DMMI-dimers are formed in aqueous media if the reaction is mediated by a triplet sensitizer, thioxanthone-2,7- disulfonate, each constituting a covalent junction between the precursor chains.[19,20]

mesoscopic additives into one common, rapidly curing polymer matrix[8,12,16,17] or by using fundamentally different materials on both sides.[13,14] By contrast, Janus microparticles which exhibit very specific, well-defined modifications on a molecular level have not to date been produced with droplet microfluidics.

An excellent strategy to circumvent this limitation is to form the preparticle drops from semidilute solutions of prefabricated precursor polymers rather than from monomers and to solidify these drops through polymer-analogous gelation rather than by monomer chain-growth gelation. This approach separates the particle formation from the synthesis of the polymer material and allows each to be controlled independently; it thus combines the control of microfluidic droplet templating with the flexibility of preparative polymer chemistry, thus allowing Janus microparticles to be formed from preconfigured precursors with precisely determined type and degree of molecular functionalization. However, the key element of this idea is that Janus microgels can be produced from macromolecular precursors, which has not to date been shown.

In this paper, we use droplet microfluidics to form Janus-shaped microgel particles from cross-linkable precursor polymers. To demonstrate the anisotropic incorporation of these precursors into the resultant microgels, we tag them with fluorescent dyes, representing arbitrary functional sites. These dyes are easy to detect and allow us to visualize the spatial distribution of the modified precursor polymers inside the microgel particles. We also take advantage of the control offered by the microfluidic droplet templating to fabricate hollow microcapsules with two different sides (Janus shells), and we extend our approach by complexing Janus microgels made from macromolecular precursors with a ferromagnetic additive, thus allowing for remote actuation of the microgels.

Results and Discussion

To realize our concept, we proceed in three steps: First, we prepare a set of cross-linkable precursor polymers; we use derivatives of poly(*N*-isopropylacrylamide) (pNIPAAm), because this polymer is highly configurable due to its solubility in a variety of solvents, both polar and nonpolar, which allows its functionalization either by copolymerization or through polymer-analogous modification.[18] To model an arbitrary modification of these precursors, we tag a fraction of them with two different

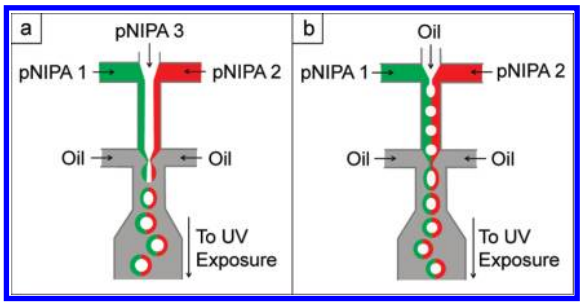

Figure 1. Formation of Janus microgels and microshells. (a) Schematic of a microfluidic device forming aqueous droplets from three independent semidilute pNIPAAm solutions. Right after droplet break-up, the center phase (colorless pNIPAAm) is assembled in the core of the droplets, whereas the left- and right-flowing phases (green- and red-tagged pNIPAAm) form a Janus-shaped shell. (b) Operating the device in a modified way yields oil−water−oil double emulsions with Janus-shaped middle phases. Curing these droplets forms hollow Janus shells. All microchannels used in this work have a width of 100 μm at the first cross-junction and 150 μm at the second cross-junction, along with a uniform height of either 130 or 170 μm.

fluorescent dyes. Then, we use microfluidic devices to form Janus-shaped drops from semidilute solutions of these precursors. Finally, we solidify these drops through rapid polymer-analogous photogelation based on the selective dimerization of pendant dimethylmaleimide (DMMI) side groups, as shown in Scheme 1.[19,20]

To formulate preparticle droplets, we employ poly(dimethylsiloxane) (PDMS) microchannels with two sequential cross-junctions as fabricated by soft lithography[21] and inject three different polymer solutions through three separate inlets as sketched in Figure 1a. These three polymer phases consist of 50 g L^{-1} aqueous solutions of cross-linkable pNIPAAm (M_n = 100 000 g mol^{-1}; M_w = 200 000 g mol^{-1}; DMMI content 0.75 mol %), along with 0.5 mmol L^{-1} of a photosensitizer, thioxanthone-2,7-disulfonate (TXS), to promote the photo-cross-linking. To visualize the formation of Janus structures, we dope the polymer phases which are injected through the left and right inlets (Figure 1a) with additional 5 g L^{-1} of either a red or a green fluorescently tagged cross-linkable pNIPAAm. These tracer polymers have a similar molecular weight and DMMI content to the untagged pNIPAAm matrix material, but contain an additional amount of 0.1 mol % of either carboxyrhodamine (red dye) or Alexa Fluor 488 (green dye). By contrast, we leave the phase injected through the middle inlet unlabeled.

After their injection, the three independent streams meet at the first cross-junction, whereupon they form a laminar coflowing stream as shown schematically in Figure 1a. The tagged materials flow in the outer threads, while the untagged matrix material flows in the middle. About 500 μm downstream, the coflowing stream enters a second cross-junction where it is broken to form monodisperse droplets by flow focusing with paraffin oil which contains 2 wt % of a modified polyether−polysiloxane surfactant (ABIL EM 90, Evonik Industries, Germany). Extensive work in the literature has shown that the size of the resultant droplets can be controlled by adjusting the fluid flow rates and channel geometry;[22−24] we use flow rates which form droplets of about 140 μm diameter.

(17) Shepherd, R. F.; Conrad, J. C.; Rhodes, S. K.; Link, D. R.; Marquez, M.; Weitz, D. A.; Lewis, J. A. *Langmuir* **2006**, *22*, 8618–8622.
(18) Schild, H. G. *Prog. Polym. Sci.* **1992**, *17*, 163–249.
(19) Seiffert, S.; Oppermann, W.; Saalwaechter, K. *Polymer* **2007**, *48*, 5599–5611.
(20) Yu, X.; Corten, C.; Goerner, H.; Wolff, T.; Kuckling, D. *J. Photochem. Photobiol. A* **2008**, *198*, 34–44.
(21) McDonald, J. C.; Duffy, D. C.; Anderson, J. R.; Chiu, D. T.; Wu, H. K.; Schueller, O. J. A.; Whitesides, G. M. *Electrophoresis* **2000**, *21*, 27–40.

During the drop formation, the continuous phase flows past the growing drop; this creates a weak convective flow,[8] which slightly distorts the three-striped pattern into a core−shell-like structure with two colored hemispheres and an uncolored center, as indicated in Figure 1a. We retain this structure until the precursor polymers are cross-linked by two means: first, we limit flow within the droplets by increasing the width of the channel right behind the junction; in narrower channels, the drop would rub against the walls, and this would induce a quick-mixing recirculating flow within the drops, as proposed by Handique and Burns,[25] and first observed by the Ismagilov group.[26,27] Second, we reduce diffusive mixing within the drop by using high-molecular-weight precursor polymers instead of faster-diffusing monomers. With little flow within the droplets and limited diffusive mixing before cross-linking, our precursor drops retain three distinguishable regions.

Once formed, the Janus droplets are exposed to strong UV light to cross-link the precursor chains as illustrated in Scheme 1.[19,20] We use a strong, focused UV beam from a 100 W mercury arc lamp (Omni Cure Exfo) for this purpose. Further wavelength selection is performed by an optical filter which transmits wavelengths only in the range 300−500 nm. We focus the light onto a spot of about 0.5 cm diameter which covers part of a serpentine delay channel about 2 cm away from the second cross-junction. The light intensity in this area is measured to be about 250 mW cm^{-2} using a powermeter; at a TXS concentration of 0.5 mmol L^{-1}, this leads to droplet solidification within a few seconds. To complete the cross-linking, the particle suspension passes the same UV spot a second and a third time when flowing through the serpentine channel before exiting the device. The 2 cm spacing between the cross-junction and the irradiation area helps to avoid gelation of the cross-linkable precursor polymers in the inlets of the microfluidic device, which can result from UV light scattering inside the PDMS elastomer. To further minimize the amount of stray light inside the microfluidic device, we trim the PDMS material as much as possible, and we wrap all supply syringes and tubing with aluminum foil to avoid UV exposure of our precursor solutions prior to their emulsification.

After collecting the gel-in-oil suspensions, we remove the supernatant oil phase, wash the microgels with isopropanol, and transfer them into water, where they swell to a size of about 200 μm at room temperature. We then image them on a confocal laser scanning fluorescence microscope (Leica TCS SP5), exciting the red and green fluorescence labels with the 543 nm line of a HeNe laser and the 488 nm line of an Ar-ion laser, respectively. Detection takes place in two separate channels in the wavelength range 650−800 nm (red channel) and 493−538 nm (green channel). We observe that all the particles exhibit distinguishable red and green halves. Due to the distortion of the gelling droplets in the bends of the serpentine delay channel, some of the resultant microgels deviate from an ideal spherical shape. A way to avoid this problem is to use a wide basin channel instead of a serpentine to cure the droplets, which produces spherical microgels only.

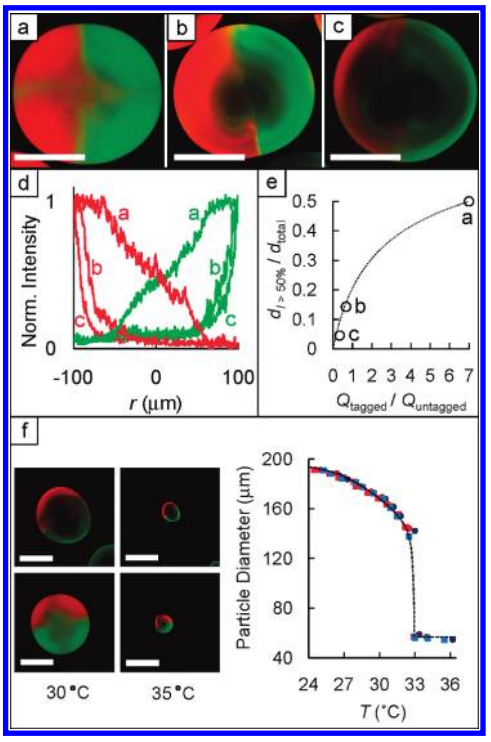

Figure 2. Characterization of pNIPAAm Janus microgels obtained from experiments as sketched in Figure 1a. Varying the flow rates of the two tagged outer polymer phases, the untagged center polymer phase, and the emulsifying oil phase from (a) 105:105:30:500 μL h^{-1} over (b) 50:50:150:500 μL h^{-1} to (c) 30:30:180:500 μL h^{-1} yields particles with different inner morphology. (d) Spatially resolved profiles of the normalized fluorescence intensity across the resultant particles (presented as moving averages of five sequential datapoints, respectively). When pixels with normalized red or green intensity greater than 0.5 are defined as part of the tagged particle shell, while those with intensity below 0.5 are defined as part of the untagged particle core, a relation between the flow rates used during the microfluidic particle production and the resultant extent of polymer interdiffusion can be derived (see text). (e) Relative diameter of the tagged shell of the microgels, $d_{I>50\%}/d_{\text{total}}$, as a function of the ratio of flow rates of the tagged and untagged polymer phases, $Q_{\text{tagged}}/Q_{\text{untagged}}$. Circles represent experimental data as derived from the intensity profiles in Panel (d), while the dotted line is calculated theoretically as detailed in the main text. (f) Thermo-responsive behavior of the Janus microgels shown in Panel (a) and (c). The left-hand micrographs show two particles with a high (upper row) and a low (lower row) content of tagged precursor polymers in a swollen (left column) and a shrunken (right column) state. The right-hand diagram details the particle diameter as a function of temperature. Circles represent the Janus particles shown in the lower row, whereas squares refer to the particles shown in the upper row. Red and blue symbols represent successive heating and cooling cycles. The dotted line was drawn manually to guide the eye. All scalebars denote 100 μm.

The distribution of the two tagged precursor polymers in the Janus particles varies as a function of the flow rates of the inner and outer phases in the three-component coflowing stream, as shown in Figure 2a−c. For these experiments, the total flow rate of all polymer phases was adjusted to 240−250 μL h^{-1}, while the continuous phase was injected at 500 μL h^{-1}. The ratio of the flow rates of the two colored to the uncolored polymer phases was varied from 105:105:30 μL h^{-1} (Figure 2a) over 50:50:150 μL h^{-1} (Figure 2b) to 30:30:180 μL h^{-1} (Figure 2c). While the separation of the red- and green-tagged precursors is marked if the flow rate of the unmodified center phase is higher than the flow rates of the

(22) Thorsen, T.; Roberts, R. W.; Arnold, F. H.; Quake, S. R. *Phys. Rev. Lett.* **2001**, *86*, 4163–4166.
(23) Garstecki, P.; Stone, H. A.; Whitesides, G. M. *Phys. Rev. Lett.* **2005**, *94*, 164501.
(24) Utada, A. S.; Fernandez-Nieves, A.; Stone, H. A.; Weitz, D. A. *Phys. Rev. Lett.* **2007**, *99*, 094502.
(25) Handique, K.; Burns, M. A. *J. Micromech. Microeng.* **2001**, *11*, 548–554.
(26) Song, H.; Tice, J. D.; Ismagilov, R. F. *Angew. Chem., Int. Ed.* **2003**, *42*, 768–772.
(27) Tice, J. D.; Song, H.; Lyon, A. D.; Ismagilov, R. F. *Langmuir* **2003**, *19*, 9127–9133.

tagged precursors (Figure 2b,c), there is less separation if the flow rate of the center phase is lower than the flow rates of the tagged phases (Figure 2a).

The main reason for cross-contamination of the two sides of the Janus microgels is diffusive intermixing of the tagged polymers in the two halves of the pregel droplets. Due to the 2 cm spacing between the droplet-forming cross-junction and the UV curing area of the microfluidic device, the droplets spend about 1 s in an unsolidified state as they flow through the delay channel. To appraise the extent of diffusive intermixing that occurs during this time, we use a confocal laser scanning microscope to perform fluorescence recovery after photobleaching (FRAP) experiments on the un-cross-linked precursor solutions used for the microgel production. These experiments are carried out and analyzed according to a method detailed elsewhere.[28,29] They show that the diffusivity of the tagged precursors can be described by a broad distribution spreading from diffusion coefficients of about 0.1 $\mu m^2 s^{-1}$ to about 50 $\mu m^2 s^{-1}$ and higher, which arises from the polydispersity of molecular weights of the tracer polymers ($M_w/M_n = 2.0$). Tracer chains from the fast end of this distribution diffuse an average linear distance of more than 10 μm in 1 s; at a droplet size of 140 μm, this gives rise to notable interdiffusion. Hence, the cross-contamination of the tagged polymers is noticeable if they are not separated by a fair amount of unmodified matrix polymer, as seen in Figure 2.

The morphology of the Janus particles depends on the relative flow rates of the colored and uncolored polymer. To quantify this dependence, we measure spatially resolved profiles of the red and green fluorescence intensity across the Janus particles, as plotted in Figure 2d. In the absence of mixing, the red and green regions would have some uniform intensities I_{max}, respectively, the uncolored region would have zero intensity, and the pixels covering the boundary between the regions would have intensity $0.5I_{max}$. Due to the presence of diffusive mixing, this boundary is smeared out; however, the pixels covering the boundary still have intensity $0.5I_{max}$, because the tagged and untagged polymers diffuse equally. Therefore, we designate the pixels with intensity above $0.5I_{max}$ as colored or "tagged" and those with intensity below $0.5I_{max}$ as "untagged". The thickness of the tagged region we call $d_{I>50\%}$ and that of the whole particle we call d_{total}. With these definitions, we plot the thickness ratio $d_{I>50\%}/d_{total}$ as a function of the flow rate ratio $Q_{tagged}/Q_{untagged}$, shown in Figure 2e. The interdependence of these two ratios follows the expected form: if we model the particle as a sphere with an untagged spherical center surrounded by a tagged, bihemispherical shell, we can straightforwardly calculate that $d_{I>50\%}/d_{total} = 1 - (1 + Q_{tagged}/Q_{untagged})^{-1/3}$, as detailed in the Supporting Information. This calculated dependence is shown as the dotted curve in Figure 2e. We obtain good agreement with our measurements without any free fitting parameters.

Since all the Janus particles shown in Figure 2 consist of pNIPAAm, they are thermoresponsive in aqueous media.[18] The mechanism of the thermoresponsive swelling and shrinking of pNIPAAm has been studied extensively,[18,30−35] and it was found that the volume phase behavior strongly depends on the chemical composition of the pNIPAAm chains: while the presence of polar moieties generally increases the lower critical solution temperature, the presence of nonpolar groups leads to its decrease.[36,37] However, since our Janus microgels are doped with not more than 5 g L^{-1} of tagged polymers, and since the degree of labeling of these polymers is only 0.1 mol %, particles with both high and low contents of tagged precursors exhibit the same, unperturbed volume phase behavior, as demonstrated in Figure 2f. In addition, a detailed look at their thermoresponsive behavior shows that these particles exhibit affine swelling and shrinking, such that their Janus pattern is unperturbed by the volume change, as also evidenced by the micrographs in Figure 2f.

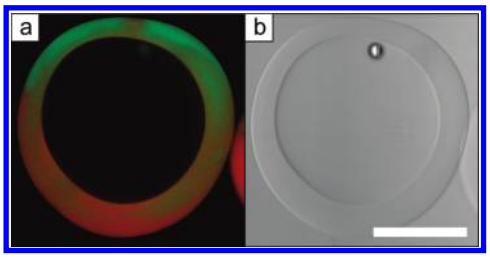

Figure 3. Fluorescence (a) and bright field (b) micrograph of a hollow Janus shell obtained from an experiment as sketched in Figure 1b, using flow rates of 40 μL h^{-1} for the inner oil phase, 120 μL h^{-1} for each of the tagged polymer phases, and 600 μL h^{-1} for the outer phase. The scale bar denotes 100 μm and applies to both panels. The small dot inside the gel shell is a former satellite droplet, which has been cured to a small microgel particle.

A simple modification of our approach to produce Janus microgels allows us to form hollow Janus shells, as sketched in Figure 1b. In this case, we produce double emulsion droplets as templates. We use the first junction of our microfluidic device to create drops of kerosene containing 2 wt % ABIL EM 90 in a continuous phase of semidilute pNIPAAm in water. The unique feature of this experiment is that we use two different coflowing pNIPAAm streams to encase the kerosene drops. In the second junction, this structured emulsion is emulsified a second time by flow focusing with paraffin oil which contains 2 wt % ABIL EM 90. This forms Janus droplets of two different pNIPAAm phases in oil, which contain kerosene droplets inside. Curing the polymer shell yields microcapsules with two distinguishable halves. A fluorescence and bright field micrograph of such a Janus shell is shown in Figure 3; it is formed with volume flow rates of 40 μL h^{-1} for the inner kerosene phase, 120 μL h^{-1} for each of the two tagged polymer phases, and 600 μL h^{-1} for the outer phase, and it exhibits an overall diameter of 230 μm and an inner core diameter of 180 μm when stored in water at room temperature. Since both the size and inner morphology of the templating double emulsion droplets can be controlled by the geometry of the microfluidic device and the flow rates of the fluids, as shown in the literature,[38−40] further control could be extended to the morphology of these Janus shells by adjustment of these experimental parameters.

A very common modification of microgel particles comprises their complexation with additives, and a very useful type of complexation is to encapsulate magnetic nanoparticles, because this allows for remote actuation of the microgels. To check whether this idea can be combined with our concept to fabricate Janus microgels from macromolecular precursors, we complex

(28) Seiffert, S.; Oppermann, W. *J. Microsc.* **2005**, *220*, 20–30.
(29) Hauser, G. I.; Seiffert, S.; Oppermann, W. *J. Microsc.* **2008**, *230*, 353–362.
(30) Tanaka, T.; Sato, E.; Hirokawa, Y.; Hirotsu, S.; Peetermans, J. *Phys. Rev. Lett.* **1985**, *55*, 2455–2458.
(31) Hirotsu, S. *J. Phys. Soc. Jpn.* **1987**, *56*, 233–242.
(32) Li, Y.; Tanaka, T. *J. Chem. Phys.* **1989**, *90*, 5161–5166.
(33) Matsuyama, A.; Tanaka, T. *J. Chem. Phys.* **1991**, *94*, 781–786.
(34) Suzuki, A.; Yoshikawa, S.; Bai, G. *J. Chem. Phys.* **1999**, *111*, 360–367.
(35) Okada, Y.; Tanaka, F. *Macromolecules* **2005**, *38*, 4465–4471.
(36) Bae, Y. H.; Okano, T.; Kim, S. W. *J. Polym. Sci., Part B: Polym. Phys.* **1990**, *28*, 923–936.
(37) Hirotsu, S.; Hirokawa, Y.; Tanaka, T. *J. Chem. Phys.* **1987**, *87*, 1392–1395.
(38) Nisisako, T.; Okushima, S.; Torii, T. *Soft Matter* **2005**, *1*, 23–27.
(39) Chu, L.-Y.; Utada, A. S.; Shah, R. K.; Kim, J.-W.; Weitz, D. A. *Angew. Chem., Int. Ed.* **2007**, *46*, 8970–8974.
(40) Seo, M.; Paquet, C.; Nie, Z.; Xua, S.; Kumacheva, E. *Soft Matter* **2007**, *3*, 986–992.

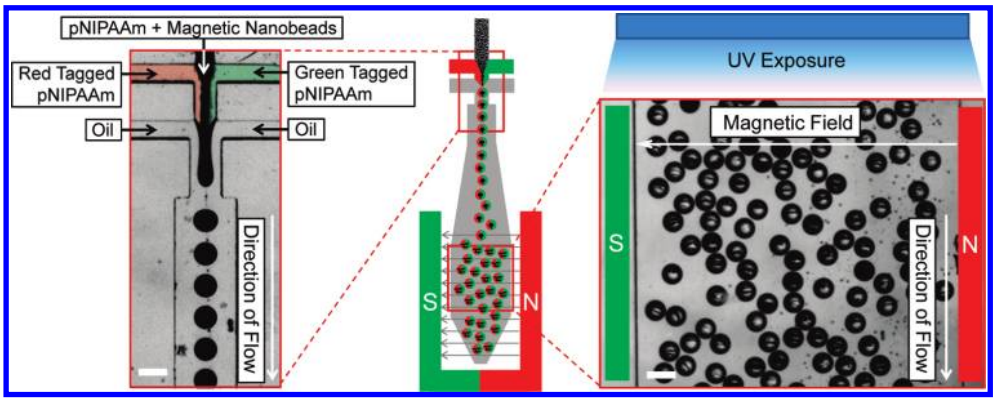

Figure 4. Fabrication of red- and green-tagged Janus-shaped pNIPAAm microgels with a permanent magnetic moment. The middle sketch shows a schematic of the microfluidic device used for this purpose. The left micrograph depicts a close-up of the upper region of the device where pregel Janus droplets that contain ferromagnetic nanoparticles are created. Note that the red and green color for the two tagged pNIPAAm phases was added digitally, because their true color is visible only by fluorescence. The right micrograph shows a close-up of the lower part of the device, a wide basin channel where the pregel droplets are cured by UV exposure. Due to the presence of an external magnetic field, as indicated in the middle sketch, the ferromagnetic nanoparticles inside the pregel drops are aligned perpendicular to the direction of flow, and hence perpendicular to the red and green color pattern. That way, red- and green-tagged Janus particles with a permanent magnetic moment are obtained. All scale bars denote 150 μm.

these microgels with a ferromagnetic additive; this idea differs from several previous reports, which focus on superparamagnetic complexation.[15,16,41] The advantage of a ferromagnetic additive is that it equips the microgels with a permanent magnetic moment of defined direction, thus offering the means to use them for advanced sensing and actuation purposes.

To realize this strategy, we perform the precursor-based microgel production with a colorless center polymer phase that is doped with 50 wt % of negatively charged ferromagnetic iron oxide nanoparticles with an average size of 300 nm (ChemiCell, Berlin, Germany), as shown in Figure 4. These magnetic nanoparticles are premagnetized by the manufacturer, and hence, they form three-dimensional agglomerates. Because these agglomerates settle rapidly, we mount both the microfluidic device and the syringe pump in a vertical position and inject the center polymer phase downward. With this configuration, droplets form without any perturbation, and the droplet size distribution is monodisperse, as seen in the right-hand micrograph in Figure 4. Moreover, the flow rates which are used to obtain droplets of a certain size are very comparable to the flow rates which lead to the same size in the absence of the ferromagnetic additive. Hence, the production efficiency of ferromagnetically complexed droplets is as high as for uncomplexed droplets, and both can be obtained as perfectly monodisperse ensembles at kilohertz rates.

Once formed, the pregel droplets enter a wide basin channel. This channel is placed between the poles of a chrome steel U-shaped magnet (Arbor Scientific, Ann Arbor, MI, U.S.A.), which orients the agglomerates of ferromagnetic nanoparticles inside the droplets along the direction of the field lines and, hence, perpendicular to both the direction of flow and the red−green color pattern, as shown in the right-hand micrograph in Figure 4. To lock this structure, we expose the droplets to strong UV light in the same area of the microfluidic device, thereby cross-linking the precursor chains.

All of the resultant microgels exhibit a red and green half, and most of them (approximately 90%) contain premagnetized, ferromagnetic nanoparticles with an alignment perpendicular to these colored halves, whereas only a small fraction of microgels (about 10%) is obtained with a less perfect orientation of their magnetic additive, as shown in Figure 5. This observation

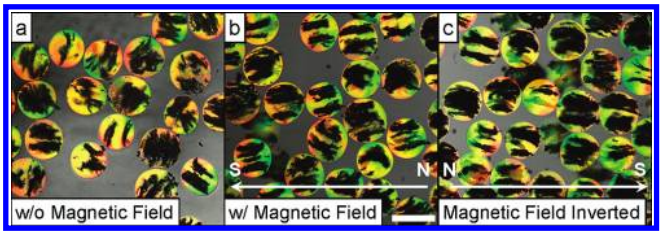

Figure 5. Red−green colored Janus particles complexed with ferromagnetic nanoparticles. Due to the presence of a homogeneous magnetic field during the microgel production (Figure 4), the ferromagnetic nanoparticles are aligned perpendicular to the red−green color pattern of the microgels. In the absence of external magnetic fields, the microgels show random orientation (a). By contrast, applying an external field orients them along the field lines (b). If the direction of the external field is inverted, the particles switch their orientation by 180° (c). The scale bar denotes 200 μm and applies to all panels.

suggests that the majority of the product microgels have a distinct, permanent magnetization perpendicular to their color pattern. Nevertheless, they do not form a notable self-organizing superstructure when stored in the absence of external magnetic fields, as seen in Figure 5a; instead, the orientation of their red and green halves is a random pattern. However, we are able to align these microgels if we apply an external magnetic field. This experimental feature is demonstrated in Figure 5b, which shows a section of the same sample as shown in Figure 5a after placing it between the poles of a U-shaped magnet. In this case, all the red halves are oriented to the left side of the micrograph (south pole of the external magnetic field), whereas all the green halves point to the right side (north pole of the external magnetic field). When the orientation of the external magnetic field is reversed, the microgel particles rotate by 180°, as shown in Figure 5c, and as also demonstrated in a movie in the electronic Supporting Information. This observation is evidence that the microgels exhibit a permanent, directed magnetic moment. To substantiate this result, we use vibrating sample magnetometry to characterize the ferromagnetically complexed gels in a dry state, as detailed in the Supporting Information. The mass magnetization of the microgel samples shows a hysteresis loop with a coercivity of 8.4×10^{-3} T, a remanence of 1.0 A m^2 kg^{-1}, a mass saturation magnetization of 19 A m^2 kg^{-1}, and an initial mass susceptibility

(41) Hwang, D. K.; Dendukuri, D.; Doyle, P. S. *Lab Chip* **2008**, *8*, 1640–1647.

of 1.5×10^{-4} m^3 kg^{-1}. After their alignment in an external magnetic field, the orientation of the magnetically complexed microgels remains even when the external field is removed. This is because the microgel particles exhibit sizes of several hundred micrometers and, hence, are not subject to Brownian motion, such that they do not relax back into a random orientation.

Conclusions

The polymer-analogous microgel formulation technique presented in this paper is a versatile way of producing micrometer-sized hydrogel particles with an asymmetric modification. Since the precursor polymers used to form them can be functionalized prior to the microgel formation, highly controlled microfluidic templating can be combined with the great flexibility of preparative polymer chemistry, allowing bifunctional or anisotropic microgels to be produced with precisely determined properties. Loading these particles with functional additives, such as ferromagnetic nanoparticles, combines the asymmetric modification of the polymer shell with the functionality of the additive. Since the microfluidic devices used in this work are made by soft lithography, the method can be scaled up, offering the potential to produce larger quantities of new anisotropic microparticles.

Acknowledgment. We thank Prof. Caroline A. Ross and Helena Liu (Massachusetts Institute of Technology) for their assistance with vibrating sample magnetometry. This work was supported by the NSF (DMR-1006546) and the Harvard MRSEC (DMR-0820484). S.S. received funding from the German Academy of Sciences Leopoldina (BMBF-LPD 9901/8-186), which is gratefully acknowledged.

Supporting Information Available: Full experimental details, a movie showing the magnetic actuation of the magnetized microgels, as well as AutoCAD and PDF files of the photomasks used for soft lithographic device fabrication. This material is available free of charge via the Internet at http://pubs.acs.org.